

Stable Carbon Isotope Signature of Methane Released from Phytoplankton

Thomas Klintzsch¹, Hannah Geisinger¹, Anna Wieland¹, Gerald Langer², Gernot Nehrke³, Mina Bizic⁴, Markus Greule⁵, Katharina Lenhart⁶, Christian Borsch⁷, Moritz Schroll⁵, and Frank Keppler⁸

¹Institute of Earth Sciences

²The Marine Biological Association of the United Kingdom

³Alfred-Wegener-Institute for Polar and Marine Research

⁴Leibniz Institute of Freshwater Ecology and Inland Fisheries

⁵Heidelberg University

⁶University of Applied Sciences

⁷Gießen University

⁸University of Heidelberg

February 20, 2023

Abstract

Aquatic ecosystems play an important role in global methane cycling and many field studies have reported methane supersaturation in the oxic surface mixed layer (SML) of the ocean and in the epilimnion of lakes. The origin of methane formed under oxic condition is hotly debated and several pathways have recently been offered to explain the ‘methane paradox’. In this context, stable isotope measurements have been applied to constrain methane sources in supersaturated oxygenated waters. Here we present stable carbon isotope signatures for six widespread marine phytoplankton species, three haptophyte algae and three cyanobacteria, incubated under laboratory conditions. The observed isotopic patterns implicate that methane formed by phytoplankton might be clearly distinguished from methane produced by methanogenic archaea. Comparing results from phytoplankton experiments with isotopic data from field measurements, suggests that algal and cyanobacterial populations may contribute substantially to methane formation observed in the SML of oceans and lakes.

Hosted file

955430_0_art_file_10713663_rq4zml.docx available at <https://authorea.com/users/587513/articles/625160-stable-carbon-isotope-signature-of-methane-released-from-phytoplankton>

Stable Carbon Isotope Signature of Methane Released from Phytoplankton

T. Klintzsch^{1,2}, H. Geisinger², A. Wieland², G. Langer³, G. Nehrke⁴, M. Bizic⁵, M. Greule²,
K. Lenhart⁶, C. Borsch⁷, M. Schroll² and F. Keppler^{2,8}

¹Department for Plant Nutrition, Gießen University, Gießen, Germany.

²Institute of Earth Sciences, Heidelberg University, Heidelberg, Germany.

³Institute of Environmental Science and Technology (ICTA), Universitat Autònoma de Barcelona, Barcelona, Spain.

⁴Marine Biogeosciences, Alfred Wegener Institut – Helmholtz-Zentrum für Polar- und Meeresforschung, Bremerhaven, Germany.

⁵Leibniz Institute of Freshwater Ecology and Inland Fisheries (IGB), Stechlin, Germany

⁶Professorship of Botany, Limnology and Ecotoxicology, University of Applied Sciences, Bingen.

⁷Institute of Nutritional Science, Gießen University, Gießen, Germany.

⁸Heidelberg Center for the Environment (HCE), Heidelberg University, Heidelberg, Germany.

Corresponding authors: Thomas Klintzsch (thomas.klintzsch@umwelt.uni-giessen.de), Frank Keppler (frank.keppler@geow.uni-heidelberg.de).

Key Points:

- Stable carbon isotope values of methane emitted from six phytoplankton cultures incubated in the laboratory
- Isotope fractionation between methane source signature and biomass of widespread algal and cyanobacterial species
- Isotopic patterns of methane released by phytoplankton may be clearly distinguished from methane formed by methanogenic archaea

25 **Abstract**

26 Aquatic ecosystems play an important role in global methane cycling and many field studies
27 have reported methane supersaturation in the oxic surface mixed layer (SML) of the ocean and in
28 the epilimnion of lakes. The origin of methane formed under oxic condition is hotly debated and
29 several pathways have recently been offered to explain the ‘methane paradox’. In this context,
30 stable isotope measurements have been applied to constrain methane sources in supersaturated
31 oxygenated waters. Here we present stable carbon isotope signatures for six widespread marine
32 phytoplankton species, three haptophyte algae and three cyanobacteria, incubated under
33 laboratory conditions. The observed isotopic patterns implicate that methane formed by
34 phytoplankton might be clearly distinguished from methane produced by methanogenic archaea.
35 Comparing results from phytoplankton experiments with isotopic data from field measurements,
36 suggests that algal and cyanobacterial populations may contribute substantially to methane
37 formation observed in the SML of oceans and lakes.

38

39 **Plain Language Summary**

40 Methane plays an important role in atmospheric chemistry and physics as it contributes to global
41 warming and to the destruction of ozone in the stratosphere. Knowing the sources and sinks of
42 methane in the environment is a prerequisite for understanding the global atmospheric methane
43 cycle but also to better predict future climate change. Measurements of the stable carbon isotope
44 composition of carbon – the ratio between the heavy and light stable isotope of carbon – help to
45 identify methane sources in the environment and to distinguish them from other formation
46 processes. We identified the carbon isotope fingerprint of methane released from phytoplankton
47 including algal and cyanobacterial species. The observed isotope signature improves our
48 understanding of methane cycling in the surface layers of aquatic environments helping us to
49 better estimate methane emissions to the atmosphere.

50

51 **1 Introduction**

52

53 Methane (CH₄) plays an important role in atmospheric chemistry and physics as it contributes to
54 global warming and the destruction of ozone in the stratosphere. Aquatic environments including
55 oceans, lakes, rivers, estuaries, and wetlands have recently been estimated to contribute to
56 around half of annual global CH₄ emissions to the atmosphere (Rosentreter et al., 2021),
57 although a large portion of the CH₄ produced in these individual ecosystems is oxidized by
58 methanotrophic bacteria in the sediment or water column before escaping to the atmosphere
59 (Reeburgh, 2007; Weber et al., 2019). Despite CH₄ losses through oxidation and release at the
60 water surface to the atmosphere, numerous field studies have shown CH₄ supersaturation in the
61 oxic surface mixed layer (SML) of the ocean (e.g. Karl et al., 2008; Kolomijeca et al., 2022;
62 Scranton & Brewer, 1977; Scranton & Farrington, 1977; Sosa et al., 2019; Taenzer et al., 2020;
63 Weber et al., 2019) and in the epilimnion of lakes (e.g. Donis et al., 2017; Grossart et al., 2011;
64 Günthel et al., 2019; Hartmann et al., 2020; Tang et al., 2016; Thottathil et al., 2022).
65 Maintaining the CH₄ supersaturation state requires frequent CH₄ production in the oxygenated
66 water column, though it has been postulated for decades that microbial CH₄ production by
67 methanogenic archaea is prevented by oxygen. Several sources and processes have recently been

68 proposed to explain the so called “methane paradox” occurring in oxic waters in oceans and
69 lakes which we summarize in the following. (1) Methane might be produced by photochemical
70 degradation of the algal metabolite dimethyl sulfide (DMS) or acetone and chromophore organic
71 matter (Bange & Uher, 2005; Li et al., 2020; Zhang et al., 2015). (2) Methane is formed by
72 microbes including (a) methanogenic archaea in anoxic microsites (de Angelis & Lee, 1994; Karl
73 & Tilbrook, 1994; Oremland, 1979; Schmale et al., 2018; Stawiarski et al., 2019; Zindler et al.,
74 2013), (b) bacterial degradation of the algal metabolites dimethylsulfonium propionate (DMSP)
75 and its degradation products dimethyl sulfoxide (DMSO) and DMS (Damm et al., 2010; Damm
76 et al., 2008; Florez-Leiva et al., 2013), (c) N₂-fixing bacteria, carrying Fe-only nitrogenase
77 (Zheng et al., 2018), (e) bacterial conversion of methylamine (Wang et al., 2021) and (d)
78 bacterial degradation of methyl phosphonates (MPn) via the C-P lyase reaction pathway, with
79 MPn serving as an alternative source of P under phosphate-limiting conditions (del Valle & Karl,
80 2014; Karl et al., 2008; Metcalf et al., 2012; Repeta et al., 2016; Taenzer et al., 2020). (3)
81 Phytoplankton produces CH₄ *per se* (Bižić et al., 2020a; Ernst et al., 2022; Klintzsch et al., 2019;
82 Klintzsch et al., 2020; Lenhart et al., 2016; McLeod et al., 2021), (4) and specifically for surface
83 waters of lakes physical transport processes from shallow water zones to the open surface waters
84 (Encinas Fernández et al., 2016, Peeters et al., 2019). For a more detailed overview of the
85 different sources and processes please refer to recent review articles (e.g. Bižić et al., 2020b;
86 Bižić, 2021; DelSontro et al., 2018; Liu et al., 2022; Reeburgh, 2007; Tang et al., 2016).

87 Interestingly, a very recent study (Perez-Coronel & Beman, 2022) that applied freshwater
88 incubation experiments under different treatments suggested multiple sources act simultaneously
89 to explain aerobic CH₄ production in aquatic environments. Several recent studies have applied
90 stable isotope techniques to better constrain the origin and fate of CH₄ in lakes (Einzmann et al.,
91 2022; Hartmann et al., 2020; Taenzer et al., 2020; Thottathil & Prairie, 2021; Thottathil et al.,
92 2022; Tsunogai et al., 2020). The stable carbon isotope ratio (¹³C/¹²C) of CH₄ (expressed as
93 δ¹³C-CH₄ values) depends on the production, degradation, and transport processes within the
94 aquatic system. Thus, a comprehensive temporal and spatial δ¹³C-CH₄ data set of the water
95 column is useful to disentangle sources and sinks. Their inclusion together with CH₄
96 concentration data allows for improved modelling of the regional and global CH₄ budget
97 (Sherwood et al., 2017). As phytoplankton might contribute to CH₄ production in both oxic
98 marine and freshwater environments, we measured δ¹³C-CH₄ values from phytoplankton
99 including three widespread marine haptophyte algal, and three cyanobacteria species. The six
100 phytoplankton species were incubated under controlled laboratory conditions and the apparent
101 isotopic fractionation between phytoplanktonic CH₄ and biomass was calculated. The importance
102 of the observed isotopic patterns for our understanding of aquatic CH₄ cycling is discussed in
103 relation to recent results from field experiments and to well-known isotope patterns of biotic and
104 abiotic CH₄ sources.

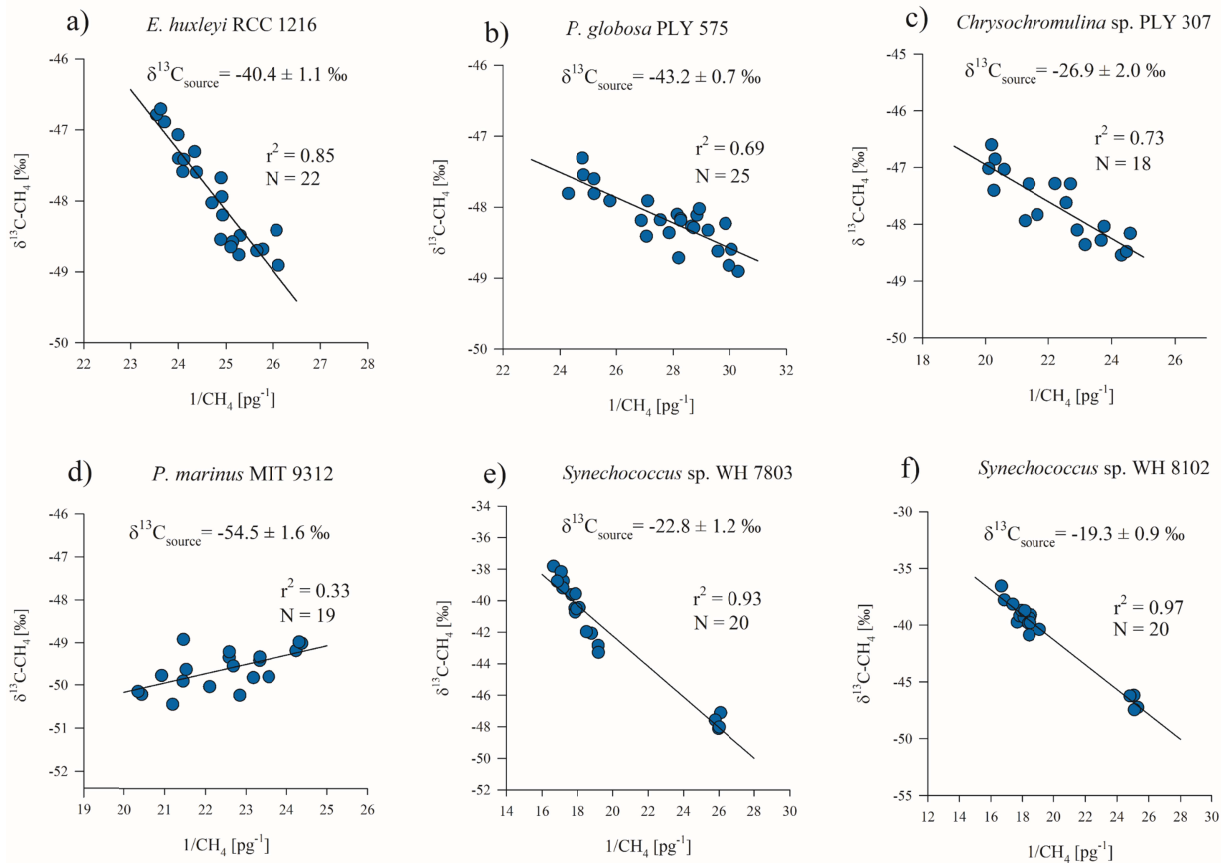
105 2 Results and Discussion

106 2.1 Stable carbon isotope signature and isotopic fractionation of CH₄ emitted from 107 phytoplankton.

108 Six phytoplankton cultures were cultivated under sterile conditions, including three different
109 marine algal species (haptophytes) and three cyanobacteria species. We determined CH₄ mass
110 and δ¹³C-CH₄ values in the cultures’ headspace at the end of the incubation period. In addition,
111 stable carbon isotope values of particulate organic matter (δ¹³C-POC) were measured (a detailed

112 methodical description is given in the Supporting Information Text S1-Text S5 and Figure S1).
113 At the end of the incubation period, the CH₄ mass in the headspace of all studied cultures
114 increased compared to the medium control group. The latter remained at the initial measured
115 atmospheric background CH₄ levels (all culture vessels were closed in atmospheric air and thus
116 contained background CH₄). The amount of CH₄ produced correlated positively with the amount
117 of initial inoculated phytoplankton biomass (Figure S2). Simultaneously, the $\delta^{13}\text{C-CH}_4$ values in
118 five cultures shifted towards to more positive values with increasing CH₄ production when
119 compared to the control group, i.e., atmospheric background values, while a shift towards more
120 negative values was observed for one culture only. To determine the isotopic source signature of
121 CH₄ ($\delta^{13}\text{C-CH}_4_{\text{source}}$) of the phytoplankton cultures the Keeling plot method (Keeling, 1958)
122 was used as described in the Supporting Information (Text S2). Figure 1 shows the Keeling plots
123 for each species in which the intersection of the extrapolated regression between $\delta^{13}\text{C-CH}_4$
124 values and the inverse CH₄ mass yields the CH₄ source signatures. Five cultures produced CH₄
125 that was clearly enriched in ¹³C relative to the $\delta^{13}\text{C-CH}_4$ values of atmospheric CH₄ ($\approx -47\%$)
126 yielding $\delta^{13}\text{C-CH}_4_{\text{source}}$ values ranging between -19% and -43% (Figure 1, a, b, c, e, f), while
127 a slight depletion in ¹³C relative to atmospheric CH₄ was found only for *Prochlorococcus* strain
128 (-54% ; Figure 1, d). Based on the discrepancy between $\delta^{13}\text{C-CH}_4_{\text{source}}$ values (Figure 1) and
129 the $\delta^{13}\text{C-POC}$ values (Table S1) the apparent stable carbon isotopic fractionation during CH₄
130 formation ($\epsilon_{\text{CH}_4/\text{POC}}$) was calculated for each phytoplankton species. The corresponding isotopic
131 fractionations are shown for each species in Figure 2. The observed negative values for $\epsilon_{\text{CH}_4/\text{POC}}$
132 ranging from $-29.8 \pm 1.7\%$ to $-1.4 \pm 0.7\%$ exhibited a ¹³C depletion of released CH₄ when
133 compared to the biomass expressed as POC, with the exception of *Synechococcus* WH8102,
134 where no fractionation occurred ($+0.5 \pm 1.0\%$). Thus, CH₄ formation by phytoplankton
135 followed the general isotope fractionation rule that in kinetic reactions the lighter isotopes tend to
136 react faster, resulting in a ¹³C-depleted product compared to the substrate (see e.g., Fry, 2006).
137 However, based on the degree of fractionation, the calculated $\epsilon_{\text{CH}_4/\text{POC}}$ values obviously suggest
138 two different CH₄ formation patterns of the phytoplankton species. On the one hand, CH₄
139 formation by *E. huxleyi*, *P. globosa*, and *Prochlorococcus* resulted in a substantial depletion of
140 ¹³C in the formed CH₄ compared to their $\delta^{13}\text{C-POC}$ values, with an average fractionation of -23
141 $\pm 4\%$. On the other hand, *Chrysochromulina* sp. and both *Synechococcus* strains showed
142 average $\epsilon_{\text{CH}_4/\text{POC}}$ values of $-1 \pm 1\%$ (Figure 2). Thus, the $\delta^{13}\text{C}$ values of CH₄ emitted by these
143 strains are nearly the same as those measured for POC. Currently, we can only speculate about
144 the reasons of the observed different $\epsilon_{\text{CH}_4/\text{POC}}$ values. It is known that different metabolic
145 pathways are accompanied by specific kinetic isotope fractionation that leads to specific $\delta^{13}\text{C}$
146 values of the cellular compounds (e.g., see Hayes, 2001). Thus, the different $\epsilon_{\text{CH}_4/\text{POC}}$ values
147 calculated for the six investigated species may indicate that these organisms used different
148 pathways and/or precursor compounds to produce CH₄. This is well known for CH₄ formation
149 pathways of methanogenic archaea: the CO₂-reducing pathway fractionates significantly stronger
150 against ¹³C than the acetoclastic pathway, with apparent isotopic fractionations of around -49%
151 and -19% , respectively (see Conrad, 2005 and references therein). Analogously, the CH₄
152 formation by marine algae, with isotopic fractionations of *P. globosa* and *E. huxleyi* (-22.6 ± 0.9
153 $\%$ and $-17.9 \pm 1.2\%$) distinct from those of *Chrysochromulina* sp. ($-2.1 \pm 2.5\%$) might be the
154 result of conversion of different CH₄ precursor compounds. This hypothesis is supported by
155 recent studies (Klintzsch et al., 2019; Lenhart et al., 2016), showing that methylated sulfur
156 compounds such as DMS, DMSO, methionine sulfoxide and methionine are potential CH₄
157 precursor compounds in marine algae. It has been shown that the investigated algal species

158 produce these compounds in mM cellular concentrations (Liss et al., 1994; Sunda et al., 2002)
 159 with the synthesis of these compounds requiring individual enzymatic steps (Bullock et al., 2017;
 160 Stefels, 2000). Therefore, a different isotopic composition of the methyl precursors might cause
 161 different isotope fractionation in CH₄ produced by phytoplankton as observed in our study
 162 (Figure 2). This might also explain the larger differences in isotopic fractionation between
 163 phytoplankton cultures even though $\delta^{13}\text{C}$ -POC values were similar (Table S1). Please note that
 164 within this study it was not possible to extract potential methyl precursor compounds such as
 165 DMS or DMSO from the incubation experiments and measure their $\delta^{13}\text{C}$ values.



166

167 **Figure 1.** Keeling plots from three haptophytes (a, b, c) and *Cyanobacteria* species (d, e, f). The
 168 calculated $\delta^{13}\text{C}\text{-CH}_4_{\text{source}}$ values of each species are given by the extrapolated intercept with the
 169 y axis CH₄ ($1/[\text{CH}_4] = 0$). The correlation between CH₄ mass (given as reciprocal) and the
 170 $\delta^{13}\text{C}\text{-CH}_4$ values of all incubations is shown in detail for each plot. N refers to the total number
 171 of observations from independent incubation experiments.

172

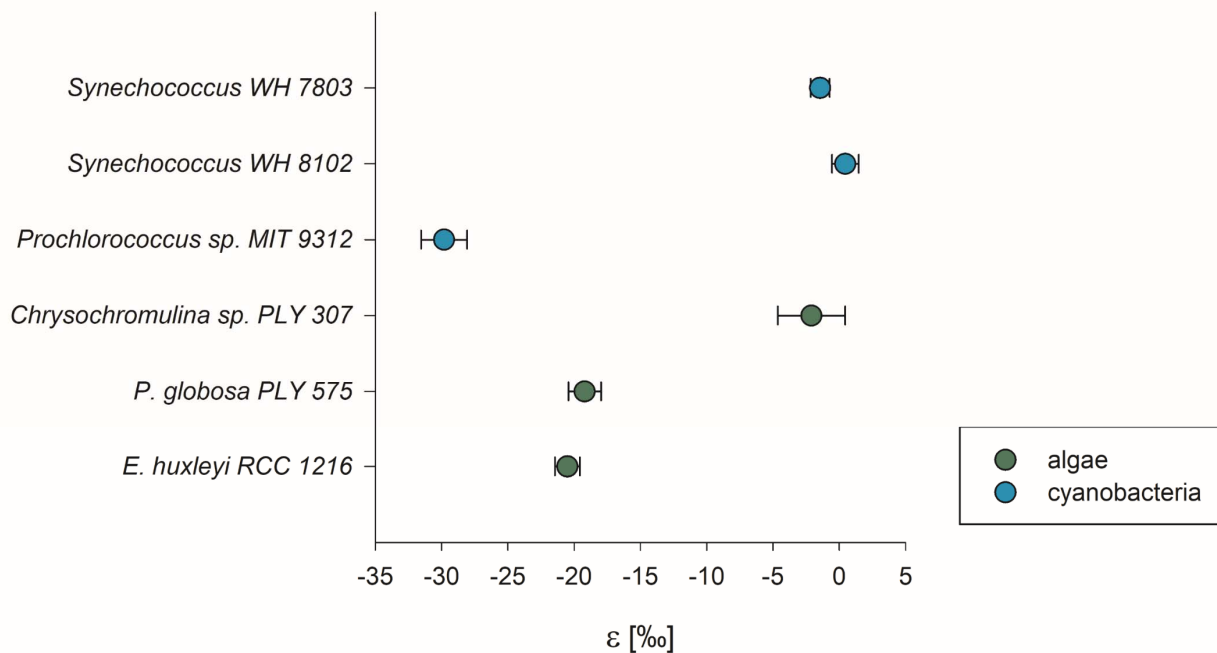
173 *Cyanobacteria* including the investigated genera *Synechococcus* and *Prochlorococcus* have been
 174 shown to produce methylated sulfur compounds but in extremely low-intracellular
 175 concentrations (Corn et al., 1996; McParland & Levine, 2019). In contrast, MPn associated with
 176 esters are common in many bacteria strains (Metcalf et al., 2012). Methylphosphonates can be
 177 metabolized by several marine bacteria as an alternative phosphorus source via the C-P lyase

178 pathway whereby CH₄ is released (del Valle & Karl, 2014; Karl et al., 2008; Repeta et al., 2016;
179 Taenzer et al., 2020). Taenzer et al. (2020) showed that the MPn cleaving by freshwater and
180 marine bacterial strains leads to marginal isotopic fractionation between substrate MPn and
181 produced CH₄ with average ϵ values of 1.3 ‰. Based on the observed isotopic pattern, the
182 research team concluded that MPn is a likely source of CH₄ in the surface waters of the Pacific
183 Ocean (station ALOHA, Taenzer et al., 2020). However, the MPn related CH₄ formation
184 pathway might be less relevant for the experiments conducted in our study because of the
185 following reasons. All of the investigated strains lack the C-P lyase gene (Bižić et al., 2020a) and
186 the phosphate rich conditions of the culture medium would, if present, inhibit C-P lyase gene
187 expression (Bižić et al., 2020a). Although Yao et al. (2022) showed for some freshwater bacterial
188 cultures that C-P lyase gene expression was not completely inhibited by phosphorus, the addition
189 of MPn was mandatory to induce C-P lyase gene expression. In addition, Sosa et al. (2021)
190 showed that *Prochlorococcus* processes MPn to formate rather than to CH₄. Thus, in our
191 experiments the cleavage of MPn is rather unlikely to explain the observed CH₄ formation.
192 Consequently, there must be other mechanisms of CH₄ formation in addition to the C-P lyase
193 pathway. According to Ernst et al. (2022), oxic CH₄ formation might occur in living organisms
194 from all domains of life when sulfur or nitrogen-methylated compounds are converted to CH₄ by
195 a Fenton-type reaction via formation of methyl radicals. This reaction might cause relatively
196 small fractionations between biomass and CH₄, because radical-induced reactions are typically
197 associated with small fractionations between precursors and reaction products (Morasch et al.,
198 2004). Consequently, the ROS-driven pathway suggested by Ernst et al. (2022), might explain
199 the small fractionations observed in our experiments for the three phytoplankton species
200 *Chrysochromulina* sp., *Synechococcus* WH8102 and WH7803 (on average -1 ± 1 ‰, Figure 2).
201 On the other hand, the larger calculated isotopic fractionations of -29.8 ± 1.7 ‰ to -17.9 ± 1.2 ‰
202 for *Prochlorococcus* MIT 9312, *E. huxleyi* and *P. globosa*, respectively, imply that different
203 methyl precursor substrates and/or pathways were involved in the CH₄ formation by the three
204 phytoplankton species.

205 Even though the reaction pathways and the specific circumstances leading to the observed
206 fractionation patterns between POC and CH₄ of the six investigated species remain unclear, the
207 results show, for the first time the range of $\epsilon_{\text{CH}_4/\text{POC}}$ values directly obtained from phytoplankton
208 cultures. The fractionations between POC and CH₄ might help to trace back CH₄ formation in
209 field studies, which will be discussed in greater detail in the section 2.3 below. To accomplish
210 the presented dataset of marine algal and cyanobacteria species we provide further
211 $\delta^{13}\text{C}-\text{CH}_4_{\text{source}}$ values of freshwater and terrestrial cyanobacteria which were calculated from
212 culture experiments performed in previous laboratory experiments (Bižić et al., 2020a). The data
213 is provided in the Supporting Information (Figure S3; Text S6) and are considered in the
214 discussion section below.

215

216



217

218 **Figure 2.** Apparent isotopic fractionation between phytoplanktonic POC and released CH₄.
 219 Values are the mean of replicated culture experiments. Error bars show the standard error.

220

221 2.2 The stable carbon isotope pattern of CH₄ released from phytoplankton compared with
 222 other well-known CH₄ sources

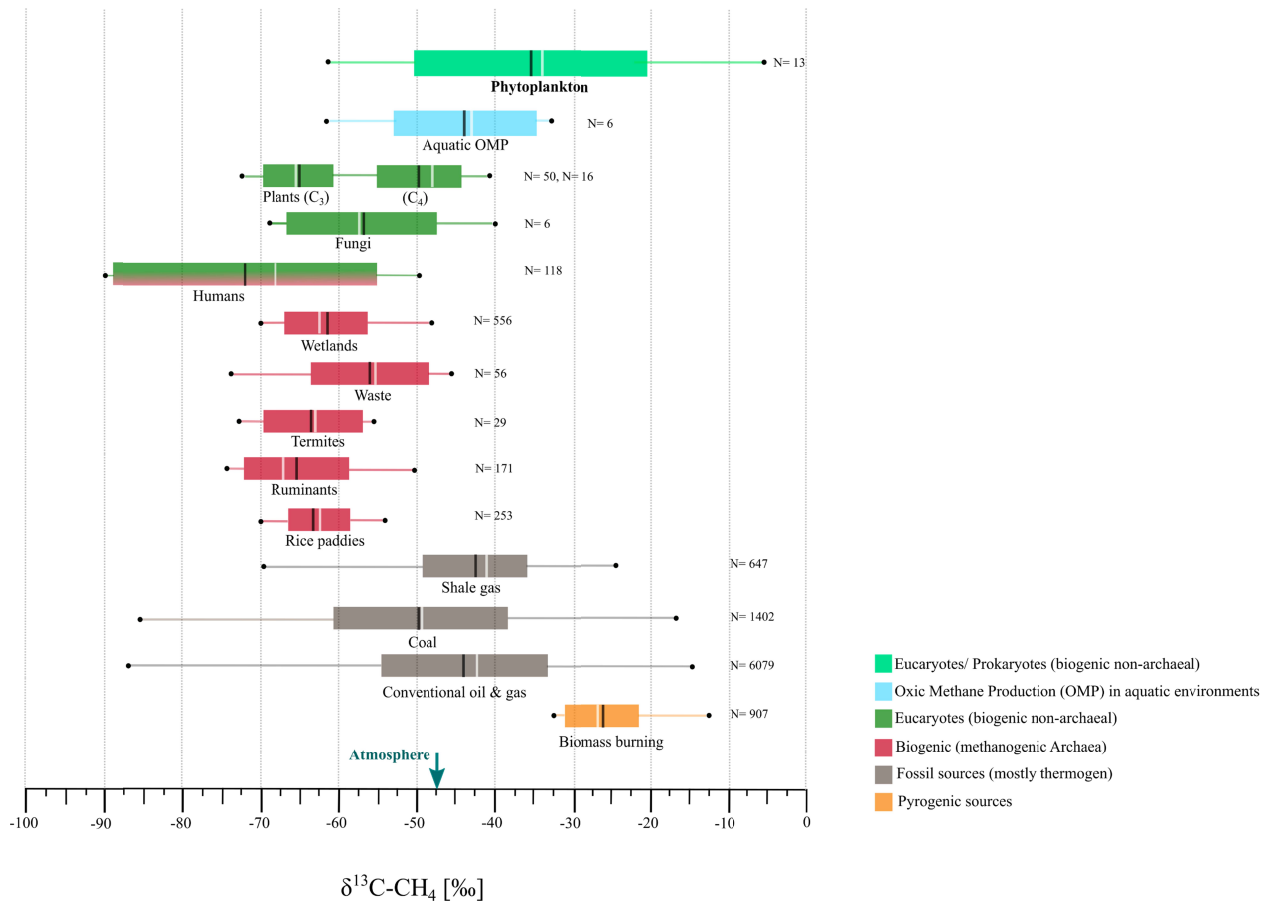
223 Global CH₄ monitoring is usually based on measurements of CH₄ mixing ratios, i.e.,
 224 quantification of CH₄ emissions, while a growing number of studies include measurements of
 225 δ¹³C-CH₄ values in order to better constrain the strengths of different sources in context of total
 226 emissions (e.g., Allen, 2016; Dlugokencky et al., 2011; Fletcher & Schaefer, 2019; Houweling et
 227 al., 2017; Menoud et al., 2022; Nisbet & Weiss, 2010). Ranges of measured δ¹³C-CH₄ values
 228 have been reported for conventional sources which might be classified into thermogenic (from
 229 geological processes), pyrogenic (from biomass burning) and biogenic (from methanogenic
 230 archaea) origin (Saunio et al., 2020). Recently, δ¹³C-CH₄ values from eukaryotic sources
 231 including plants, fungi and humans have been reported (Keppler et al., 2006, 2016; Schroll et al.,
 232 2020; Vigano et al., 2009) which we categorize as “biogenic non-archaeal” CH₄ formation
 233 processes.

234 In Figure 3, we compare the already known δ¹³C-CH₄_{source} patterns from various sources with
 235 those observed from phytoplanktonic cultures obtained in our study. Pyrogenic CH₄, produced
 236 during biomass burning exhibits mean δ¹³C-CH₄ values of -26.2 ± 4.8 ‰ and thus is typically
 237 highly enriched in ¹³C compared to atmospheric CH₄ (≈ -47 ‰). Thermogenic δ¹³C-CH₄ values,
 238 produced from buried biomass in the Earth’s crust, shows median δ¹³C-CH₄ values of -49.8 ±
 239 11.2 ‰, -42.5 ± 6.7 ‰ and -44.0 ± 10.7 ‰ for coal, shale gas and conventional oil and gas,
 240 respectively (Sherwood et al., 2017). These values are very similar to atmospheric values. Both
 241 source categories, pyrogenic and thermogenic, are often referred to as abiotic sources because a
 242 metabolic activity is not directly involved in their CH₄ formation process – although the

243 precursor compounds are derived from organic matter (Boros & Keppler, 2018). In contrast,
244 biotic CH₄, including traditional pathways (from methanogens) and novel discovered non-
245 archaeal sources, is directly linked to biological metabolic processes, and released CH₄ tends to
246 be ¹³C-depleted relative to atmospheric values (Figure 3). Biogenic CH₄, produced by
247 methanogenic archaea in anoxic environments, typically ranges from -72 to -47 ‰ (Sherwood et
248 al., 2017), depending on its individual source category. The $\delta^{13}\text{C-CH}_4$ values emitted from
249 biogenic non-archaeal sources such as plants and fungi lie between -70 ‰ and -45 ‰ and thus
250 are almost in the same range as those $\delta^{13}\text{C-CH}_4$ values reported for methanogenic archaea. $\delta^{13}\text{C-}$
251 CH₄ values directly emitted from plants depend on the autotrophic carbon fixation pathway
252 (Keppler et al., 2006; Viganò et al., 2009), as the C₃ and C₄ photosynthetic pathway controls the
253 isotopic composition of biomass, which in turn influences the $\delta^{13}\text{C-CH}_4$ values from plants (see
254 $\delta^{13}\text{C-CH}_4$ values of C₃ and C₄ plants in Figure 3). Similarly, $\delta^{13}\text{C-CH}_4$ values of CH₄ released by
255 fungi is related to the $\delta^{13}\text{C}$ values of the growth substrate (Schroll et al., 2020). In human breath,
256 a $\delta^{13}\text{C-CH}_4_{\text{source}}$ values ranging from -90 ‰ to -49.3 ‰ were observed (Keppler et al., 2016).
257 Traditionally, human CH₄ production was considered to exclusively arise from methanogenic
258 archaea living in the gastrointestinal tract (Bond et al., 1971). However, recent investigations
259 (Keppler et al., 2016; Polag & Keppler, 2018, 2022) suggest that CH₄ is also formed
260 endogenously in human cells. Thus, $\delta^{13}\text{C-CH}_4$ values measured from human breath might
261 include both pathways which are currently difficult to distinguish. The CH₄ production by
262 marine algae and cyanobacteria investigated in this study is categorized into “biogenic non-
263 archaeal CH₄”, as the CH₄ is formed under oxic conditions by the metabolism of the members
264 from the domain *Eukaryote* and *Prokaryote*. The $\delta^{13}\text{C-CH}_4_{\text{source}}$ values of marine
265 phytoplankton, ranging from -54.5 ‰ to -19.3 ‰, showed mostly less negative $\delta^{13}\text{C-CH}_4$ values
266 (median -33.7 ‰) when compared to both atmospheric values and previously described biogenic
267 non-archaeal CH₄ sources (e.g., plants and fungi). The tendency of less negative values is in line
268 with the $\delta^{13}\text{C-CH}_4_{\text{source}}$ values of the two terrestrial and five limnic cyanobacteria (median -33.8
269 ‰) ranging between -61.4 ‰ to -5.4 ‰ (Figure S3).

270 The observed $\delta^{13}\text{C-CH}_4_{\text{source}}$ values from phytoplankton considerably extend the range of
271 biogenic non-archaeal CH₄ towards less negative $\delta^{13}\text{C-CH}_4$ values of up to -5.4 ‰. Therefore,
272 biotic and abiotic CH₄ source categories are less clearly delimited due to their $\delta^{13}\text{C-CH}_4$ values
273 isotopic signature when taking those of phytoplankton into account. Figure 3 shows that the
274 range of measured $\delta^{13}\text{C-CH}_4$ values for methanogenic archaea has little overlap with $\delta^{13}\text{C-}$
275 CH₄_{source} values of phytoplankton. Therefore, phytoplanktonic CH₄ might be clearly
276 distinguished from CH₄ produced by methanogenic archaea based on their $\delta^{13}\text{C-CH}_4_{\text{source}}$
277 values. However, at the ecosystem scale, even distinguishing between two different co-occurring
278 methanogenic sources based on their $\delta^{13}\text{C-CH}_4$ values is complex, requiring knowledge of
279 additional parameters as discussed in Conrad (2005). Furthermore, microbial CH₄ oxidation is a
280 widespread feature in oxic and anoxic environments which might change the initial $\delta^{13}\text{C-}$
281 CH₄_{source} value. The CH₄ oxidation reduces the ¹²C content, resulting in an increase of the ¹³C
282 content in the remaining CH₄ pool (Barker & Fritz, 1981). In recent field studies microbial CH₄
283 oxidation were considered for calculating $\delta^{13}\text{C-CH}_4_{\text{source}}$ values of oxic CH₄ production by mass
284 balance within the epilimnion of lakes (Hartmann et al., 2020; Thottathil et al., 2022). These
285 researcher hypothesized the occurrence of oxic CH₄ production by phytoplankton because CH₄
286 formation was spatially associated with phytoplankton blooms and calculated $\delta^{13}\text{C-CH}_4$ values
287 were less negative than would be expected from methanogenic archaea. In this context, it is
288 important to note that the range of phytoplanktonic $\delta^{13}\text{C-CH}_4_{\text{source}}$ values obtained in our

289 laboratory study largely overlaps with $\delta^{13}\text{C-CH}_4$ values previously calculated for aquatic oxic
 290 CH_4 production derived from field investigations of several lakes (Hartmann et al., 2020;
 291 Sasakawa et al., 2008; Thottathil et al., 2022). Therefore, our isotopic results support the
 292 hypothesis that in aquatic environments under certain conditions direct formation of CH_4 by
 293 phytoplankton might fully or partly explain the observed elevated CH_4 concentrations in oxic
 294 surface layers which often is described as the “methane paradox”. In addition, the
 295 $\delta^{13}\text{C-CH}_4_{\text{source}}$ values of phytoplankton complement our understanding of isotopic carbon
 296 source signatures of CH_4 in the environment. In the context of the aquatic CH_4 paradox, the
 297 results could help to differentiate between CH_4 produced by methanogenic archaea in anoxic
 298 microsites, the intestinal tract of zooplankton or sedimentary sources, and those produced from
 299 phytoplankton as for example recently applied by Einzmann et al. (2022) to constrain sources
 300 and sinks of CH_4 in a small lake in Southern Germany.



301 $\delta^{13}\text{C-CH}_4$ [‰]

302 **Figure 3.** Typical range of $\delta^{13}\text{C-CH}_4_{\text{source}}$ values of pyrogenic, fossil, biogenic and eukaryotic
 303 CH_4 sources. The box marks the SD and whiskers the min-max value. The mean and median are
 304 given by the black and white stripe within the box respectively. $\delta^{13}\text{C-CH}_4$ values of the
 305 thermogenic, pyrogenic and biogenic sources represent values from many individual studies
 306 summarized by Sherwood et al. (2017) which is currently the most comprehensive data set with
 307 respect to CH_4 source signature values. The $\delta^{13}\text{C-CH}_4$ value of plants were taken from Keppler et
 308 al. (2006) and Vigano et al. (2009) and the ones of fungi and humans from Keppler et al. (2016)
 309 and Schroll et al. (2020). $\delta^{13}\text{C-CH}_4$ values calculated for aquatic oxic CH_4 production (OMP)
 310 derived from lake and ocean field studies are taken from Thottathil et al. (2022), Holmes et al.

311 (2000) and Sasakawa et al. (2008). The $\delta^{13}\text{C}-\text{CH}_4_{\text{source}}$ value of phytoplankton are summarized
 312 from both section 2.1 and Figure S3. Detailed information regarding classification of CH_4 can be
 313 found in Boros & Keppler (2018), Conrad (2009), Etiope & Sherwood Lollar (2013), Kirschke et
 314 al. (2013) and Saunio et al. (2016).
 315

316 2.3 Potential contribution of phytoplankton to CH_4 supersaturated SML

317 To assess the potential environmental relevance of the isotope data of phytoplankton obtained by
 318 the laboratory experiments, we compiled the available isotope data for POC and $\delta^{13}\text{C}-\text{CH}_4$ values
 319 of CH_4 supersaturated SMLs reported from field studies of oceans and lakes (e.g., Forster et al.,
 320 2009; Grossart et al., 2011; Günthel et al., 2019; Hartmann et al., 2020; Scranton & Brewer,
 321 1977; Weber et al., 2019).

322 We assume that $\delta^{13}\text{C}-\text{CH}_4$ values of phytoplankton depend on the $\delta^{13}\text{C}-\text{POC}$ values according to
 323 equation 1

$$324 \delta^{13}\text{C}-\text{CH}_4 = \delta^{13}\text{C}-\text{POC} + \Delta^{13}\text{C}_{\text{CH}_4/\text{POC}}, \quad 1$$

325
 326 where $\Delta^{13}\text{C}_{\text{CH}_4/\text{POC}}$ is the isotopic difference associated with CH_4 release from POC ($\epsilon_{\text{CH}_4/\text{POC}} \approx$
 327 $\Delta^{13}\text{C}_{\text{CH}_4/\text{POC}} = \delta^{13}\text{C}-\text{CH}_4 - \delta^{13}\text{C}-\text{POC}$). Therefore, $\delta^{13}\text{C}-\text{POC}$ values and the isotope difference
 328 associated with the release of CH_4 from POC are fundamental for the evaluation of laboratory
 329 $\delta^{13}\text{C}-\text{CH}_4$ values with regard to their environmental relevance. A comprehensive compilation of
 330 $\delta^{13}\text{C}-\text{POC}$ data of the world ocean has been provided by Goericke and Fry (1994). Most $\delta^{13}\text{C}-$
 331 POC values range from -28 ‰ to -18 ‰ with even lower values in the polar regions (see
 332 Goericke & Fry, 1994 and references inside). In this study, the $\delta^{13}\text{C}-\text{POC}$ values of the
 333 investigated phytoplankton species range from ≈ -26 ‰ to -19 ‰ (Table S1) and thus reflect the
 334 range of $\delta^{13}\text{C}-\text{POC}$ values typically found in marine environments. However, it should be noted,
 335 that the $\delta^{13}\text{C}-\text{POC}$ values from oceanic POC samples are considered to reflect the carbon of the
 336 phytoplankton and are therefore often used as its proxy, but may also contain carbon from
 337 heterotrophic organisms or detritus, which may have distinct $\delta^{13}\text{C}-\text{POC}$ values (Hansman &
 338 Sessions, 2016; Marty & Planas, 2008). An alternative biomarker and possibly better proxy for
 339 haptophytes in the ocean, are alkenone lipids synthesized by the haptophytes *E. huxleyi* and
 340 *Gephyrocapsa oceanica* (e.g., Bidigare et al., 1997; Popp et al., 1989). $\delta^{13}\text{C}-\text{POC}$ values of
 341 haptophytes, estimated from alkenone lipids, globally range from -28.7 ± 1.2 ‰ to -21.5 ± 1.6 ‰
 342 with the Santa Monica Basin and Peru Upwelling Zone showing the lowest and highest values,
 343 respectively (Table 3 in Bidigare et al., 1997). The reported range fits well with $\delta^{13}\text{C}-\text{POC}$ data
 344 of the three haptophyte species investigated in our study (Table S1).

345 Based on the reported $\delta^{13}\text{C}-\text{POC}$ values of natural haptophyte populations from the literature and
 346 $\Delta^{13}\text{C}_{\text{CH}_4/\text{POC}}$ values established from our laboratory-grown haptophytes, using equation 1, natural
 347 haptophyte populations could generate $\delta^{13}\text{C}-\text{CH}_4$ values ranging from -49.2 ‰ to -23.6 ‰ within
 348 the SML. Analogously, by using the $\delta^{13}\text{C}-\text{POC}$ values reported by Goericke & Fry (1994) for
 349 cyanobacterial populations and $\Delta^{13}\text{C}_{\text{CH}_4/\text{POC}}$ values calculated from our experiments lead to $\delta^{13}\text{C}-$
 350 CH_4 values ranging from -56 ‰ to -22 ‰.

351 The next step is to compare the theoretical calculated data with field observations. Yet, only a
352 few studies reporting $\delta^{13}\text{C-CH}_4$ values of CH_4 dissolved in the SML of seawater are available in
353 the literature (Florez-Leiva et al., 2013; Holmes et al., 2000; Sasakawa et al., 2008; Yoshikawa
354 et al., 2014), showing that the SML seawater is typically supersaturated with ^{13}C -enriched CH_4 ,
355 relative to atmospheric values of around -47 ‰. It should be emphasized that $\delta^{13}\text{C-CH}_4$ values
356 measured in the SML do not necessarily reflect their isotopic source value, since microbial CH_4
357 oxidation, input from lateral or sub-thermocline water masses and atmospheric release
358 potentially modulate $\delta^{13}\text{C-CH}_4$ values (Reeburgh, 2007; Holmes et al., 2000; Sasakawa et al.,
359 2008). For this reason, isotopic CH_4 source values need to be estimated by application of
360 thorough mass balances. In this way, the $\delta^{13}\text{C-CH}_4_{\text{source}}$ values maintaining CH_4 supersaturation
361 were estimated to be -42.5 ‰ to -43 ‰ and -33 ‰ within the SML of the tropical and
362 northwestern North Pacific respectively (Holmes et al., 2000; Sasakawa et al., 2008). These
363 values are in good agreement with the above estimated range of $\delta^{13}\text{C-CH}_4$ source values for the
364 six phytoplankton species investigated in our study. Thus, natural populations of phytoplankton
365 are likely to be responsible for the ^{13}C -enriched CH_4 reported for the SML by Holmes et al.
366 (2000) and Sasakawa et al. (2008).

367 Similar to the observation of oxic CH_4 production in the surface waters of oceans, there has been
368 a controversial discussion about the occurrence of CH_4 formation in the epilimnion of lakes
369 (Bižić et al., 2020b; Encinas Fernández et al., 2016; Grossart et al., 2011; Günthel et al., 2020;
370 Hartmann et al., 2020; Tang et al., 2014, 2016; Peeters et al., 2019). A comprehensive data set of
371 $\delta^{13}\text{C-CH}_4$ values of lake water has recently been provided for Lake Stechlin in Germany
372 (Hartmann et al., 2020) and five lakes in Canada (Thottathil et al., 2022).

373 Based on the stable carbon isotope mass balance of CH_4 produced and the correlation between
374 CH_4 and chlorophyll, the research teams suggested phytoplanktonic CH_4 production as the most
375 likely source to explain the CH_4 oversaturation in the epilimnion during spring and summer. This
376 hypothesis has recently been strongly supported by Perez-Coronel & Beman (2022) that
377 associated aerobic CH_4 production with (bacterio)chlorophyll metabolism and photosynthesis.
378 $\delta^{13}\text{C-CH}_4_{\text{source}}$ values of oxic CH_4 production in surface water were distinct from the much more
379 negative $\delta^{13}\text{C-CH}_4$ values measured in sediment pore water produced by methanogenic archaea
380 (Thottathil et al., 2022; Hartmann et al., 2020). In the epilimnion of Lake Stechlin in Germany
381 $\delta^{13}\text{C-CH}_4_{\text{source}}$ values from oxic CH_4 formation during spring/summer were found to be less
382 negative than -50 ‰ (Hartmann et al., 2020). A similar isotope pattern, i.e. an enrichment of ^{13}C
383 in CH_4 relative to other sources, was also found by Thottathil et al. (2022). In four out of the five
384 studied Canadian Shield lakes, $\delta^{13}\text{C-CH}_4_{\text{source}}$ values of oxic CH_4 production, leading to CH_4
385 oversaturated surface waters during the summer period, ranged from -47 ‰ to -38 ‰. Therefore,
386 a contribution of phytoplankton to the observed $\delta^{13}\text{C-CH}_4_{\text{source}}$ values in the oversaturated oxic
387 surface waters is greatly supported by our laboratory culture experiments as we found
388 $\delta^{13}\text{C-CH}_4_{\text{source}}$ values of the thirteen phytoplankton species ranging from -61.4 ‰ to -5.4 ‰
389 (median value -33.8 ‰). These data include five freshwater phytoplankton species (Figure S3)
390 grown with $\delta^{13}\text{C-DIC}$ values \approx -4 ‰ (Text S7), which is within the natural various of $\delta^{13}\text{C-DIC}$
391 values in lakes (Bade et al., 2004). Thus, based on the $\delta^{13}\text{C-DIC}$ values, and assuming a
392 dependence between the isotopic composition of the carbon precursor and the $\delta^{13}\text{C-CH}_4_{\text{source}}$
393 values as described above, the $\delta^{13}\text{C-CH}_4_{\text{source}}$ values of laboratory grown freshwater
394 phytoplankton could be ecologically relevant. Although microbial consumption of CH_4 might be
395 also involved in increasing $\delta^{13}\text{C-CH}_4$ values in the surface waters we strongly suggest that direct

396 formation of CH₄ by phytoplankton contributes substantially to the oxic CH₄ formation in the
397 epilimnion of lakes during the growth period of these organisms.

398 **5 Conclusions**

399 Further insights into the CH₄ formation by phytoplankton were provided by determining stable
400 carbon isotopic fractionation ($\epsilon_{\text{CH}_4/\text{POC}}$ values) and source signatures of CH₄ emitted by three
401 marine haptophyte algal and three cyanobacterial species. The observed isotopic fractionation
402 suggests that different source substrates of CH₄ and/or pathways were involved in the CH₄
403 formation by the investigated species. The isotopic patterns suggest that in the absence of abiotic
404 and thermogenic CH₄ sources, CH₄ released by phytoplankton can be clearly distinguished from
405 CH₄ produced by methanogenic archaea, as phytoplankton exhibits significantly less negative
406 $\delta^{13}\text{C}\text{-CH}_4$ values. Based on the comparison of stable isotope data from phytoplankton
407 experiments with isotope data reported from field measurements in aquatic environments, we
408 conclude that algal and cyanobacterial populations may indeed contribute to the CH₄ observed in
409 the SML of oceans and lakes. However, more isotopic data than currently available is required to
410 better distinguish between different CH₄ sources and sinks in aquatic systems. In this context,
411 future applications of two-dimensional isotope studies including $\delta^{13}\text{C}$ and $\delta^2\text{H}$ values and even
412 clumped isotope techniques but also in combination with metagenomic and metatranscriptomic
413 data might be promising tools to allow for better differentiation between sources and sinks of
414 CH₄.

415

416 **Conflict of Interest**

417 The authors declare no conflicts of interest relevant to this study.

418 **Acknowledgments**

419 We thank Bernd Knape, Stefan Rheinberger and the ORCAS-Team at Heidelberg University for
420 technical support that helped to produce this dataset. F.K. was supported by the German
421 Research Foundation (DFG; Grants KE 884/8-2, KE 884/11-1 and KE 884/16-2).

422

423 **Open Research**

424 The data of this article will be made available after review but before publication via heiDATA,
425 which is an institutional repository for research data of the Heidelberg University of the UFZ. A
426 doi (digital object identifier) will be assigned and included in the last version of the manuscript.

427

428 **References**

- 429 Allen, G. (2016). Rebalancing the global methane budget. *Nature*, 538(7623), 46-48.
430 <https://doi.org/10.1038/538046a>
- 431 Bange, H. W., & Uher, G. (2005). Photochemical production of methane in natural waters: implications for its
432 present and past oceanic source. *Chemosphere*, 58(2), 177-183.
- 433 Bade, D. L., Carpenter, S. R., Cole, J. J., Hanson, P. C., & Hesslein, R. H. (2004). Controls of $\delta^{13}\text{C}$ -DIC in lakes:
434 Geochemistry, lake metabolism, and morphometry. *Limnology and Oceanography*, 49(4), 1160-1172.
435 <https://aslopubs.onlinelibrary.wiley.com/doi/abs/10.4319/lo.2004.49.4.1160>
- 436 Barker, J. F., & Fritz, P. (1981). Carbon isotope fractionation during microbial methane oxidation. *Nature*,
437 293(5830), 289-291. <https://doi.org/10.1038/293289a0>
- 438 Bidigare, R. R., Fluegge, A., Freeman, K. H., Hanson, K. L., Hayes, J. M., Hollander, D., et al. (1997). Consistent
439 fractionation of ^{13}C in nature and in the laboratory: Growth-rate effects in some haptophyte algae. *Global*
440 *Biogeochemical Cycles*, 11(2), 279-292.
441 <https://agupubs.onlinelibrary.wiley.com/doi/abs/10.1029/96GB03939>
- 442 Bižić, M., Grossart, H.-P., & Ionescu, D. (2020). Methane Paradox. In *eLS* (pp. 1-11).
- 443 Bižić, M., Klintzsch, T., Ionescu, D., Hindiyeh, M. Y., Günthel, M., Muro-Pastor, A. M., et al. (2020). Aquatic and
444 terrestrial cyanobacteria produce methane. *Science Advances*, 6(3), eaax5343.
445 <https://advances.sciencemag.org/content/advances/6/3/eaax5343.full.pdf>
- 446 Bizic, M., Phytoplankton photosynthesis: an unexplored source of biogenic methane emission from oxic
447 environments, *Journal of Plankton Research*, Volume 43, Issue 6, November/December 2021, Pages 822–
448 830, <https://doi.org/10.1093/plankt/fbab069>
- 449 Bond, J. H., Jr., Engel, R. R., & Levitt, M. D. (1971). Factors influencing pulmonary methane excretion in man. An
450 indirect method of studying the in situ metabolism of the methane-producing colonic bacteria. *J Exp Med*,
451 133(3), 572-588.
- 452 Boros, M., & Keppler, F. (2018). Chapter 8 Production and Signaling of Methane. In *Gasotransmitters* (pp. 192-
453 234): The Royal Society of Chemistry.
- 454 Boros, M., & Keppler, F. (2018). Production and Signaling of Methane. *Gasotransmitters*, 12, 192.
- 455 Bullock, H. A., Luo, H., & Whitman, W. B. (2017). Evolution of Dimethylsulfoniopropionate Metabolism in Marine
456 Phytoplankton and Bacteria. *Frontiers in Microbiology*, 8(637). Review.
457 <https://www.frontiersin.org/article/10.3389/fmicb.2017.00637>
- 458 Conrad, R. (2005). Quantification of methanogenic pathways using stable carbon isotopic signatures: a review and a
459 proposal. *Organic Geochemistry*, 36(5), 739-752.
460 <http://www.sciencedirect.com/science/article/pii/S0146638004002566>
- 461 Conrad, R. (2009). The global methane cycle: recent advances in understanding the microbial processes involved.
462 *Environmental Microbiology Reports*, 1(5), 285-292.
- 463 Corn, M., Belviso, S., Partensky, F., Simon, N., & Christaki, U. (1996). Origin and Importance of Picoplanktonic
464 DMSP. In R. P. Kiene, P. T. Visscher, M. D. Keller, & G. O. Kirst (Eds.), *Biological and Environmental*
465 *Chemistry of DMSP and Related Sulfonium Compounds* (pp. 191-201). Boston, MA: Springer US.
- 466 Damm, E., Helmke, E., Thoms, S., Schauer, U., Nöthig, E., Bakker, K., & Kiene, R. P. (2010). Methane production
467 in aerobic oligotrophic surface water in the central Arctic Ocean. *Biogeosciences*, 7(3), 1099-1108.
468 <http://www.biogeosciences.net/7/1099/2010/>
- 469 Damm, E., Kiene, R. P., Schwarz, J., Falck, E., & Dieckmann, G. (2008). Methane cycling in Arctic shelf water and
470 its relationship with phytoplankton biomass and DMSP. *Marine Chemistry*, 109(1-2), 45-59. Article.
- 471 de Angelis, M. A., & Lee, C. (1994). Methane production during zooplankton grazing on marine phytoplankton.
472 *Limnology and Oceanography*, 39(6), 1298-1308.
- 473 del Valle, D. A., & Karl, D. M. (2014). Aerobic production of methane from dissolved water-column
474 methylphosphonate and sinking particles in the North Pacific Subtropical Gyre. *Aquatic Microbial*
475 *Ecology*, 73(2), 93-105. <http://www.int-res.com/abstracts/ame/v73/n2/p93-105/>
- 476 DelSontro, T., Beaulieu, J. J., & Downing, J. A. (2018). Greenhouse gas emissions from lakes and impoundments:
477 Upscaling in the face of global change. *Limnology and Oceanography Letters*, 3(3), 64-75.
478 <https://aslopubs.onlinelibrary.wiley.com/doi/abs/10.1002/lol2.10073>
- 479 Dlugokencky, E. J., Nisbet, E. G., Fisher, R., & Lowry, D. (2011). Global atmospheric methane: budget, changes
480 and dangers. *Philosophical Transactions of the Royal Society A: Mathematical, Physical and Engineering*
481 *Sciences*, 369(1943), 2058-2072. <https://royalsocietypublishing.org/doi/abs/10.1098/rsta.2010.0341> %X

- 482 Donis, D., Flury, S., Stöckli, A., Spangenberg, J. E., Vachon, D., & McGinnis, D. F. (2017). Full-scale evaluation of
483 methane production under oxic conditions in a mesotrophic lake. *Nature communications*, 8(1), 1661.
- 484 Einzmann, T., Schroll, M., Kleint, J. F., Greule, M., & Keppler, F. (2022). Application of concentration and 2-
485 dimensional stable isotope measurements of methane to constrain sources and sinks in a seasonally
486 stratified freshwater lake. *Frontiers in Environmental Science*, 10. Original Research.
487 <https://www.frontiersin.org/articles/10.3389/fenvs.2022.865862>
- 488 Encinas Fernández, J., Peeters, F., & Hofmann, H. (2016). On the methane paradox: Transport from shallow water
489 zones rather than in situ methanogenesis is the major source of CH₄ in the open surface water of lakes.
490 *Journal of Geophysical Research: Biogeosciences*, 121(10), 2717-2726.
491 <https://agupubs.onlinelibrary.wiley.com/doi/abs/10.1002/2016JG003586>
- 492 Ernst, L., Steinfeld, B., Barayeu, U., Klintzsch, T., Kurth, M., Grimm, D., et al. (2022). Methane formation driven
493 by reactive oxygen species across all living organisms. *Nature*, 603(7901), 482-487.
494 <https://doi.org/10.1038/s41586-022-04511-9>
- 495 Etiopé, G., & Sherwood Lollar, B. (2013). Abiotic methane on Earth. *Reviews of Geophysics*, 51(2), 276-299.
- 496 Fletcher, S. E. M., & Schaefer, H. (2019). Rising methane: A new climate challenge. *Science*, 364(6444), 932-933.
- 497 Florez-Leiva, L., Damm, E., & Fariás, L. (2013). Methane production induced by dimethylsulfide in surface water
498 of an upwelling ecosystem. *Progress in oceanography*, 112, 38-48.
- 499 Forster, G., Upstill-Goddard, R. C., Gist, N., Robinson, C., Uher, G., & Woodward, E. M. S. (2009). Nitrous oxide
500 and methane in the Atlantic Ocean between 50 N and 52 S: latitudinal distribution and sea-to-air flux. *Deep
501 Sea Research Part II: Topical Studies in Oceanography*, 56(15), 964-976.
- 502 Fry, B. (2006). *Stable isotope ecology* (Vol. 521): Springer.
- 503 Goericke, R., & Fry, B. (1994). Variations of marine plankton $\delta^{13}\text{C}$ with latitude, temperature, and dissolved CO₂
504 in the world ocean. *Global Biogeochemical Cycles*, 8(1), 85-90.
505 <https://agupubs.onlinelibrary.wiley.com/doi/abs/10.1029/93GB03272>
- 506 Grossart, H.-P., Frindte, K., Dziallas, C., Eckert, W., & Tang, K. W. (2011). Microbial methane production in
507 oxygenated water column of an oligotrophic lake. *Proceedings of the National Academy of Sciences*,
508 108(49), 19657-19661. <http://www.pnas.org/content/108/49/19657>.
- 509 Günthel, M., Donis, D., Kirillin, G., Ionescu, D., Bizic, M., McGinnis, D. F., et al. (2019). Contribution of oxic
510 methane production to surface methane emission in lakes and its global importance. *Nature
511 communications*, 10(1), 5497. <https://doi.org/10.1038/s41467-019-13320-0>
- 512 Günthel, M., Klawonn, I., Woodhouse, J., Bižić, M., Ionescu, D., Ganzert, L., et al. (2020). Photosynthesis-driven
513 methane production in oxic lake water as an important contributor to methane emission. *Limnology and
514 Oceanography*, n/a(n/a). <https://doi.org/10.1002/lno.11557>. <https://doi.org/10.1002/lno.11557>
- 515 Hansman, R. L., & Sessions, A. L. (2016). Measuring the in situ carbon isotopic composition of distinct marine
516 plankton populations sorted by flow cytometry. *Limnology and Oceanography: Methods*, 14(2), 87-99.
517 <https://aslopubs.onlinelibrary.wiley.com/doi/abs/10.1002/lom3.10073>
- 518 Hartmann, J. F., Günthel, M., Klintzsch, T., Kirillin, G., Grossart, H.-P., Keppler, F., & Isenbeck-Schröter, M.
519 (2020). High Spatiotemporal Dynamics of Methane Production and Emission in Oxic Surface Water.
520 *Environmental Science & Technology*, 54(3), 1451-1463. <https://doi.org/10.1021/acs.est.9b03182>
- 521 Hayes, J. M. (2001). Fractionation of Carbon and Hydrogen Isotopes in Biosynthetic Processes*. *Reviews in
522 Mineralogy and Geochemistry*, 43(1), 225-277. <https://doi.org/10.2138/gsrmg.43.1.225>
- 523 Holmes, M. E., Sansone, F. J., Rust, T. M., & Popp, B. N. (2000). Methane production, consumption, and air-sea
524 exchange in the open ocean: An Evaluation based on carbon isotopic ratios. *Global Biogeochemical Cycles*,
525 14(1), 1-10. <https://agupubs.onlinelibrary.wiley.com/doi/abs/10.1029/1999GB001209>
- 526 Houweling, S., Bergamaschi, P., Chevallier, F., Heimann, M., Kaminski, T., Krol, M., et al. (2017). Global inverse
527 modeling of CH₄ sources and sinks: an overview of methods. *Atmos. Chem. Phys.*, 17(1), 235-256.
528 <https://acp.copernicus.org/articles/17/235/2017/>
- 529 Karl, D. M., Beversdorf, L., Bjorkman, K. M., Church, M. J., Martinez, A., & DeLong, E. F. (2008). Aerobic
530 production of methane in the sea. *Nature geoscience*, 1(7), 473-478.
- 531 Karl, D. M., & Tilbrook, B. D. (1994). Production and Transport of Methane in Oceanic Particulate Organic-Matter.
532 *Nature*, 368(6473), 732-734.
- 533 Keeling, C. D. (1958). The concentration and isotopic abundances of atmospheric carbon dioxide in rural areas.
534 *Geochimica et Cosmochimica Acta*, 13(4), 322-334.
535 <http://www.sciencedirect.com/science/article/pii/0016703758900334>
- 536 Keppler, F., Hamilton, J. T., Braß, M., & Röckmann, T. (2006). Methane emissions from terrestrial plants under
537 aerobic conditions. *Nature*, 439(7073), 187.

- 538 Keppler, F., Schiller, A., Eehalt, R., Greule, M., Hartmann, J., & Polag, D. (2016). Stable isotope and high
539 precision concentration measurements confirm that all humans produce and exhale methane. *Journal of*
540 *Breath Research*, 10(1), 016003. <http://stacks.iop.org/1752-7163/10/i=1/a=016003>
- 541 Kirschke, S., Bousquet, P., Ciais, P., Saunoy, M., Canadell, J. G., Dlugokencky, E. J., et al. (2013). Three decades
542 of global methane sources and sinks. *Nature geoscience*, 6(10), 813.
- 543 Klintzsch, T., Langer, G., Nehrke, G., Wieland, A., Lenhart, K., & Keppler, F. (2019). Methane production by three
544 widespread marine phytoplankton species: release rates, precursor compounds, and potential relevance for
545 the environment. *Biogeosciences*, 16(20), 4129-4144. <https://bg.copernicus.org/articles/16/4129/2019/>
- 546 Klintzsch, T., Langer, G., Wieland, A., Geisinger, H., Lenhart, K., Nehrke, G., & Keppler, F. (2020). Effects of
547 Temperature and Light on Methane Production of Widespread Marine Phytoplankton. *Journal of*
548 *Geophysical Research: Biogeosciences*, 125(9), e2020JG005793.
549 <https://agupubs.onlinelibrary.wiley.com/doi/abs/10.1029/2020JG005793>
- 550 Kolomijeca, A., Marx, L., Reynolds, S., Cariou, T., Mawji, E., & Boulart, C. (2022). An update on dissolved
551 methane distribution in the subtropical North Atlantic Ocean. *Ocean Sci.*, 18(5), 1377-1388.
552 <https://os.copernicus.org/articles/18/1377/2022/>
- 553 Lenhart, K., Klintzsch, T., Langer, G., Nehrke, G., Bunge, M., Schnell, S., & Keppler, F. (2016). Evidence for
554 methane production by the marine algae *Emiliania huxleyi*. *Biogeosciences*, 13(10), 3163-3174.
555 <http://www.biogeosciences.net/13/3163/2016/>
- 556 Li, Y., Fichot, C. G., Geng, L., Scarratt, M. G., & Xie, H. (2020). The Contribution of Methane Photoproduction to
557 the Oceanic Methane Paradox. *Geophysical Research Letters*, 47(14), e2020GL088362.
558 <https://agupubs.onlinelibrary.wiley.com/doi/abs/10.1029/2020GL088362>
- 559 Liss, P., Malin, G., Turner, S., & Holligan, P. (1994). Dimethyl sulphide and Phaeocystis: a review. *Journal of*
560 *Marine Systems*, 5(1), 41-53.
- 561 Liu, L.-Y., Xie, G.-J., Ding, J., Liu, B.-F., Xing, D.-F., Ren, N.-Q., & Wang, Q. (2022). Microbial methane
562 emissions from the non-methanogenesis processes: A critical review. *Science of The Total Environment*,
563 806, 151362. <https://www.sciencedirect.com/science/article/pii/S0048969721064408>
- 564 Marty, J., & Planas, D. (2008). Comparison of methods to determine algal $\delta^{13}\text{C}$ in freshwater. *Limnology and*
565 *Oceanography: Methods*, 6(1), 51-63.
566 <https://aslopubs.onlinelibrary.wiley.com/doi/abs/10.4319/lom.2008.6.51>
- 567 McLeod, A. R., Brand, T., Campbell, C. N., Davidson, K., & Hatton, A. D. (2021). Ultraviolet Radiation Drives
568 Emission of Climate-Relevant Gases From Marine Phytoplankton. *Journal of Geophysical Research:*
569 *Biogeosciences*, 126(9), e2021JG006345.
570 <https://agupubs.onlinelibrary.wiley.com/doi/abs/10.1029/2021JG006345>
- 571 McParland, E. L., & Levine, N. M. (2019). The role of differential DMSP production and community composition
572 in predicting variability of global surface DMSP concentrations. *Limnology and Oceanography*, 64(2), 757-
573 773. <https://aslopubs.onlinelibrary.wiley.com/doi/abs/10.1002/lno.11076>
- 574 Menoud, M., van der Veen, C., Lowry, D., Fernandez, J. M., Bakkaloglu, S., France, J. L., et al. (2022). New
575 contributions of measurements in Europe to the global inventory of the stable isotopic composition of
576 methane. *Earth Syst. Sci. Data*, 14(9), 4365-4386. <https://essd.copernicus.org/articles/14/4365/2022/>
- 577 Metcalf, W. W., Griffin, B. M., Cicchillo, R. M., Gao, J. T., Janga, S. C., Cooke, H. A., et al. (2012). Synthesis of
578 Methylphosphonic Acid by Marine Microbes: A Source for Methane in the Aerobic Ocean. *Science*,
579 337(6098), 1104-1107.
- 580 Morasch, B., Richnow, H. H., Vieth, A., Schink, B., & Meckenstock, R. U. (2004). Stable Isotope Fractionation
581 Caused by Glycyl Radical Enzymes during Bacterial Degradation of Aromatic Compounds. *Applied and*
582 *environmental microbiology*, 70(5), 2935-2940. [https://journals.asm.org/doi/abs/10.1128/AEM.70.5.2935-](https://journals.asm.org/doi/abs/10.1128/AEM.70.5.2935-2940.2004)
583 [2940.2004](https://journals.asm.org/doi/abs/10.1128/AEM.70.5.2935-2940.2004)
- 584 Nisbet, E., & Weiss, R. (2010). Top-down versus bottom-up. *Science*, 328(5983), 1241-1243.
- 585 Oremland, R. S. (1979). Methanogenic Activity in Plankton Samples and Fish Interstines – Mechanism for Insitu
586 Methanogenesis in Oceanic Surface Waters. *Limnology and Oceanography*, 24(6), 1136-1141.
- 587 Peeters, F., Encinas Fernandez, J., & Hofmann, H. (2019). Sediment fluxes rather than oxic methanogenesis explain
588 diffusive CH₄ emissions from lakes and reservoirs. *scientific reports*, 9(1), 243.
589 <https://doi.org/10.1038/s41598-018-36530-w>
- 590 Perez-Coronel, E., & Beman, J.M. (2022). Multiple sources of aerobic methane production in aquatic ecosystems
591 include bacterial photosynthesis. *Nature communications*, 13(1), 6454. [https://doi.org/10.1038/s41467-022-](https://doi.org/10.1038/s41467-022-34105-y)
592 [34105-y](https://doi.org/10.1038/s41467-022-34105-y)

- 593 Polag, D., & Keppler, F. (2018). Long-term monitoring of breath methane. *Science of The Total Environment*, 624,
594 69-77. <https://www.sciencedirect.com/science/article/pii/S0048969717335246>
- 595 Polag, D., & Keppler, F. (2022). COVID19-vaccination affects breath methane dynamics. *bioRxiv*,
596 2022.2007.2027.501717.
597 <https://www.biorxiv.org/content/biorxiv/early/2022/07/27/2022.07.27.501717.full.pdf>
- 598 Popp, B. N., Takigiku, R., Hayes, J. M., Louda, J. W., & Baker, E. W. (1989). The post-Paleozoic chronology and
599 mechanism of ^{13}C depletion in primary marine organic matter. *American Journal of Science*, 289(4), 436-
600 454. <https://www.ajsonline.org/content/ajs/289/4/436.full.pdf>
- 601 Reeburgh, W. S. (2007). Oceanic methane biogeochemistry. *Chemical Reviews*, 107(2), 486-513.
- 602 Repeta, D. J., Ferrón, S., Sosa, O. A., Johnson, C. G., Repeta, L. D., Acker, M., et al. (2016). Marine methane
603 paradox explained by bacterial degradation of dissolved organic matter. *Nature geoscience*, 9(12), 884.
- 604 Rosentreter, J. A., Borges, A. V., Deemer, B. R., Holgerson, M. A., Liu, S., Song, C., et al. (2021). Half of global
605 methane emissions come from highly variable aquatic ecosystem sources. *Nature geoscience*, 14(4), 225-
606 230. <https://doi.org/10.1038/s41561-021-00715-2>
- 607 Sasakawa, M., Tsunogai, U., Kameyama, S., Nakagawa, F., Nojiri, Y., & Tsuda, A. (2008). Carbon isotopic
608 characterization for the origin of excess methane in subsurface seawater. *Journal of Geophysical Research: Oceans*, 113(C3). <https://agupubs.onlinelibrary.wiley.com/doi/abs/10.1029/2007JC004217>
- 609 Saunois, M., Bousquet, P., Poulter, B., Peregon, A., Ciais, P., Canadell, J. G., et al. (2016). The global methane
610 budget 2000–2012. *Earth System Science Data*, 8(2), 697-751.
- 611 Saunois, M., Stavert, A. R., Poulter, B., Bousquet, P., Canadell, J. G., Jackson, R. B., et al. (2020). The Global
612 Methane Budget 2000–2017. *Earth Syst. Sci. Data*, 12(3), 1561-1623.
613 <https://essd.copernicus.org/articles/12/1561/2020/>
- 614 Schmale, O., Wäge, J., Mohrholz, V., Wasmund, N., Gräwe, U., Rehder, G., et al. (2018). The contribution of
615 zooplankton to methane supersaturation in the oxygenated upper waters of the central Baltic Sea.
616 *Limnology and Oceanography*, 63(1), 412-430.
- 617 Schroll, M., Keppler, F., Greule, M., Eckhardt, C., Zorn, H., & Lenhart, K. (2020). The stable carbon isotope
618 signature of methane produced by saprotrophic fungi. *Biogeosciences*, 17(14), 3891-3901.
619 <https://bg.copernicus.org/articles/17/3891/2020/>
- 620 Scranton, M. I., & Brewer, P. G. (1977). Occurrence of methane in the near-surface waters of the western
621 subtropical North-Atlantic. *Deep Sea Research*, 24(2), 127-138.
622 <http://www.sciencedirect.com/science/article/pii/0146629177905483>
- 623 Scranton, M. I., & Farrington, J. W. (1977). Methane production in the waters off Walvis Bay. *Journal of*
624 *Geophysical Research*, 82(31), 4947-4953. <http://dx.doi.org/10.1029/JC082i031p04947>
- 625 Sherwood, O. A., Schwietzke, S., Arling, V. A., & Etiope, G. (2017). Global Inventory of Gas Geochemistry Data
626 from Fossil Fuel, Microbial and Burning Sources, version 2017. *Earth Syst. Sci. Data*, 9(2), 639-656.
627 <https://essd.copernicus.org/articles/9/639/2017/>
- 628 Sosa, O. A., Casey, J. R., & Karl, D. M. (2019). Methylphosphonate Oxidation in *Prochlorococcus* Strain MIT9301
629 Supports Phosphate Acquisition, Formate Excretion, and Carbon Assimilation into Purines. *Applied and*
630 *environmental microbiology*, 85(13), e00289-00219. [https://aem.asm.org/content/aem/85/13/e00289-
631 19.full.pdf](https://aem.asm.org/content/aem/85/13/e00289-19.full.pdf)
- 632 Stawiarski, B., Otto, S., Thiel, V., Gräwe, U., Loick-Wilde, N., Wittenborn, A. K., et al. (2019). Controls on
633 zooplankton methane production in the central Baltic Sea. *Biogeosciences*, 16(1), 1-16.
- 634 Stefels, J. (2000). Physiological aspects of the production and conversion of DMSP in marine algae and higher
635 plants. *Journal of Sea Research*, 43(3), 183-197.
636 <http://www.sciencedirect.com/science/article/pii/S138511010000307>
- 637 Sunda, W., Kieber, D. J., Kiene, R. P., & Huntsman, S. (2002). An antioxidant function for DMSP and DMS in
638 marine algae. *Nature*, 418(6895), 317-320. <https://doi.org/10.1038/nature00851>
- 639 Taenzer, L., Carini, P. C., Masterson, A. M., Bourque, B., Gaube, J. H., & Leavitt, W. D. (2020). Microbial Methane
640 From Methylphosphonate Isotopically Records Source. *Geophysical Research Letters*, 47(1),
641 e2019GL085872. <https://agupubs.onlinelibrary.wiley.com/doi/abs/10.1029/2019GL085872>
- 642 Tang, K. W., McGinnis, D. F., Frindte, K., Brüchert, V., & Grossart, H.-P. (2014). Paradox reconsidered: Methane
643 oversaturation in well-oxygenated lake waters. *Limnol. Oceanogr*, 59(1), 275-284.
- 644 Tang, K. W., McGinnis, D. F., Ionescu, D., & Grossart, H.-P. (2016). Methane Production in Oxic Lake Waters
645 Potentially Increases Aquatic Methane Flux to Air. *Environmental Science & Technology Letters*, 3(6),
646 227-233. <http://dx.doi.org/10.1021/acs.estlett.6b00150>

- 648 Thottathil, S. D., & Prairie, Y. T. (2021). Coupling of stable carbon isotopic signature of methane and ebullitive
649 fluxes in northern temperate lakes. *Science of The Total Environment*, 777, 146117.
650 <https://www.sciencedirect.com/science/article/pii/S0048969721011840>
- 651 Thottathil, S. D., Reis, P. C. J., & Prairie, Y. T. (2022). Magnitude and Drivers of Oxidic Methane Production in
652 Small Temperate Lakes. *Environmental Science & Technology*, 56(15), 11041-11050.
653 <https://doi.org/10.1021/acs.est.2c01730>
- 654 Tsunogai, U., Miyoshi, Y., Matsushita, T., Komatsu, D. D., Ito, M., Sukigara, C., et al. (2020). Dual stable isotope
655 characterization of excess methane in oxidic waters of a mesotrophic lake. *Limnology and Oceanography*,
656 65(12), 2937-2952. <https://aslopubs.onlinelibrary.wiley.com/doi/abs/10.1002/lno.11566>
- 657 Vigano, I., Röckmann, T., Holzinger, R., van Dijk, A., Keppler, F., Greule, M., Brand, W.A., Geilmann, H., van
658 Weelden, H. . (2009). The stable isotope signature of methane emitted from plant material under UV
659 irradiation. *Atmospheric Environment*, 43, 5637-5646
- 660 Wang, Q., Alowafeer, A., Kerner, P., Balasubramanian, N., Patterson, A., Christian, W., et al. (2021). Aerobic
661 bacterial methane synthesis. *Proc Natl Acad Sci U S A*, 118(27).
- 662 Weber, T., Wiseman, N. A., & Kock, A. (2019). Global ocean methane emissions dominated by shallow coastal
663 waters. *Nature communications*, 10(1), 4584. <https://doi.org/10.1038/s41467-019-12541-7>
- 664 Yao, M., Henny, C., & Maresca, J. A. (2016). Freshwater Bacteria Release Methane as a By-Product of Phosphorus
665 Acquisition. *Applied and environmental microbiology*, 82(23), 6994-7003.
666 <http://www.ncbi.nlm.nih.gov/pmc/articles/PMC5103098/>
- 667 Yoshikawa, C., Hayashi, E., Yamada, K., Yoshida, O., Toyoda, S., & Yoshida, N. (2014). Methane sources and
668 sinks in the subtropical South Pacific along 17°S as traced by stable isotope ratios. *Chemical Geology*, 382,
669 24-31. <https://www.sciencedirect.com/science/article/pii/S0009254114002721>
- 670 Zhang, Y., Xie, H., & Xie, H. (2015). Photomineralization and photomethanification of dissolved organic matter in
671 Saguenay River surface water.
- 672 Zheng, Y., Harris, D. F., Yu, Z., Fu, Y., Poudel, S., Ledbetter, R. N., et al. (2018). A pathway for biological methane
673 production using bacterial iron-only nitrogenase. *Nature Microbiology*, 3(3), 281-286.
674 <https://doi.org/10.1038/s41564-017-0091-5>
- 675 Zindler, C., Bracher, A., Marandino, C. A., Taylor, B., Torrecilla, E., Kock, A., & Bange, H. W. (2013). Sulphur
676 compounds, methane, and phytoplankton: interactions along a north-south transit in the western Pacific
677 Ocean. *Biogeosciences*, 10(5), 3297-3311.

Stable Carbon Isotope Signature of Methane Released from Phytoplankton

T. Klintzsch^{1,2}, H. Geisinger², A. Wieland², G. Langer³, G. Nehrke⁴, M. Bizic⁵, M. Greule², K. Lenhart⁶, C. Borsch⁷, M. Schroll² and F. Keppler^{2,8}

¹Department for Plant Nutrition, Gießen University, Gießen, Germany.

²Institute of Earth Sciences, Heidelberg University, Heidelberg, Germany.

³The Laboratory, Citadel Hill, The Marine Biological Association of the United Kingdom, Plymouth, UK.

⁴Marine Biogeosciences, Alfred Wegener Institut – Helmholtz-Zentrum für Polar- und Meeresforschung, Bremerhaven, Germany.

⁵Leibniz Institute of Freshwater Ecology and Inland Fisheries (IGB), Stechlin, Germany

⁶Professorship of Botany, Limnology and Ecotoxicology, University of Applied Sciences, Bingen.

⁷ Institute of Nutritional Science, Gießen University, Gießen, Germany.

⁸Heidelberg Center for the Environment (HCE), Heidelberg University, Heidelberg, Germany.

Contents of this file

Text S1 to Culture and cultivation conditions.

Text S2 to The experimental set-up.

Text S3 to Determination of the stable isotope composition of the algae POC

Text S4 to Determination of CH₄ quantity using GC-FID.

Text S5 to Determination of stable carbon isotope values of CH₄ using GC-C-IRMS.

Text S6 to Determination of stable carbon isotope source values of CH₄ from previously published cyanobacterial incubation experiments.

Text S7 to Determination of $\delta^{13}\text{C}$ -DIC values.

Figure S1 to Experimental set up and the Keeling plot technique.

Figure S2 to Correlation between CH₄ production and initial inoculated phytoplankton biomass.

Figure S3 to Keeling plots of five limnic cyanobacteria (a, c, d, f, g) and two terrestrial cyanobacterial species (b, e).

Table S1 to $\delta^{13}\text{C}$ -POC [‰] values of phytoplankton species.

Introduction

The $\delta^{13}\text{C}$ -CH_{4,source} values from the three marine algae cultures (*E. huxleyi*, *Chrysochromulina* sp. and *P. globosa*) and three marine cyanobacterial cultures (*Prochlorococcus marinus* and two stains of *Synechococcus*) were determined by independent experiments using the Keeling plot technique. The stable carbon isotope composition of the phytoplankton POC ($\delta^{13}\text{C}$ -POC values) were recorded and the apparent isotope fractionation during POC and CH₄ formation was calculated. The experimental setup, measuring techniques and the calculation of the apparent fractionation are described in the following. In addition, $\delta^{13}\text{C}$ -CH_{4,source} values were determined using Keeling plots from five limnic and two terrestrial cyanobacteria incubation experiments previously published in Bižić et al. (2020). In addition, we determined the $\delta^{13}\text{C}$ -DIC values of the culture medium of these cultures. Keeling plots and a brief description of the experiments are included in these appendices.

Text S1 Culture and cultivation conditions.

The haptophyte algal species, *E. huxleyi* RCC 1216 was obtained from the Roscoff Culture Collection (<http://roscoff-culture-collection.org/>; last access: 2 December 2020) *P. globosa* PLY 575, and *Chrysochromulina* sp. PLY 307 were obtained from the Marine Biological Association of the United Kingdom (<https://www.mba.ac.uk/facilities/culture-collection> last access: 22 December 2022). *Prochlorococcus marinus* MIT 9313, *Synechococcus* WH 7803 and WH 8102 were obtained from Haifa University, Laboratory of Dr. Daniel Sher. All cultures grew in sterile, controlled laboratory conditions under a 16/8 h light-dark cycle and in sterile filtered (0.2 μm \varnothing pore size) natural North Sea seawater (sampled off Helgoland, Germany) enriched in nutrients according to F/2 medium (Guillard and Ryther, 1962). Cyanobacteria grew at 22.5 °C with a light intensity of $\approx 100 \mu\text{mol m}^{-2} \text{s}^{-1}$ and alga cultures at 20 °C with $\approx 450 \mu\text{mol m}^{-2} \text{s}^{-1}$.

Text S2 The experimental set-up

The experimental set-up for each algae and cyanobacteria species consisted of several cultivation groups that differed from each other only in their initial biomass density, resulting in a biomass dilution series. In this way, a continuous increase in headspace CH₄ mass, which is statistically ideal for the application of Keeling plots was

Text S3 Determination of the stable isotope composition of the algae POC

For the determination of the stable isotope composition of phytoplankton POC ($\delta^{13}\text{C}$ -POC values), cultures were filtered at the end of the experiment on pre-combusted (500 °C, 5 h) glass fiber filters (Whatman, GF/F 25 mm Ø filters, 0.4–0.6 µm Ø pore size). Filter samples were dried for 24 h at 50 °C and fumed with saturated hydrochloric acid to remove all inorganic carbon afterwards. To prepare the samples for the measurements, they were encapsulated in tinplate. For practical reasons, we used two different measurement systems. For representative POC values, $\geq 45\%$ of all culture flasks were determined.

The $\delta^{13}\text{C}$ -POC values of *E. huxleyi* RCC 1216, *P. globosa* PLY 575 and *Chrysochromulina* sp. PLY 307 were measured in duplicate with a mass spectrometer (ANCA-SL 20-20). Isoleucine with a $\delta^{13}\text{C}$ -POC of -12.6 ± 0.3 ‰ was used as working standard. (The mean and standard deviation is based on three measurements of working standard). All $\delta^{13}\text{C}$ -POC values were calibrated against standard material with $\delta^{13}\text{C}$ -POC of -26.4 ‰ (USGS40- standard, NIST, Gaithersburg, USA).

To determine the $\delta^{13}\text{C}$ -POC values of *P. marinus* MIT 9313, *Synechococcus* WH 7803 and WH 8102 the samples underwent total combustion at 920 °C under Helium atmosphere with additional oxygen (PyroCube, Elementar DE, Langensfeld, Germany). The CO_2 was trapped and purged from other elements oxidation products and its amount measured by thermal conductivity detection in the gas stream. $^{13}\text{C}/^{12}\text{C}$ ratios were determined in an isotope ratio mass spectrometer (Isoprime, Elementar UK, Stockport, UK) and calibrated against international standards (CH3, CH6) obtained from IAEA (Vienna, Austria). All isotope ratios were expressed as delta values ($\delta^{13}\text{C}_{\text{VPDB}}$) after Craig correction (Craig, 1957), i.e. as per mil difference in detected isotope ratios ($^{13}\text{C}/^{12}\text{C}$) against VPDB (Eq. S3).

The obtained $\delta^{13}\text{C}$ -POC and $\delta^{13}\text{C}$ - $\text{CH}_4_{\text{source}}$ values of the phytoplankton species were used to calculate the apparent isotopic fractionation (ϵ) of stable carbon isotopes between the different carbon species. The apparent isotopic fractionation during CH_4 formation ($\epsilon_{\text{CH}_4/\text{POC}}$) was calculated with regard to the algae POC due to equation S1.

$$\epsilon_{\text{CH}_4/\text{POC}} = \frac{(\delta^{13}\text{C}-\text{CH}_4 + 1)}{(\delta^{13}\text{C}-\text{POC} + 1)} - 1 \quad \text{Eq. S1}$$

The standard error of the isotopic fractionation was calculated using Gaussian error propagation by partial derivation of the individual error variables.

Text S4 Determination of CH₄ quantity using GC-FID

The CH₄ mass [ng] was determined for the entire incubation flask (i.e., CH₄ dissolved in the culture medium and CH₄ of the headspace volume). For this determination, a sample was taken from the headspace using a gas-tight syringe. Methane was analyzed using a gas chromatograph with FID detector (GC-FID, GC-14B, Shimadzu, Japan) and a 2 m column, (Ø = 3.175 mm inner diameter) packed with molecular sieve 5A 60/80 mesh (Supelco). The method was calibrated with two reference standards (2192 ppbv, 9837 ppbv CH₄ mixing ratio, average analytical standard deviation 5 ppbv and 53 ppbv, respectively, n = 3).

Prior to gas sampling, the pressure of the headspace was measured (GMSD 1.3 BA, Greisinger). The CH₄ mass was determined by its mixing ratio (x) and the ideal gas law (Equation S2)

$$m_{CH_4} = M_{CH_4} \times x_{CH_4} \frac{p \times V}{R \times T}, \quad \text{Eq. S2}$$

where M is molar mass, p is pressure, T is temperature, R is the ideal gas constant, and V is volume. The concentration of dissolved CH₄ was calculated according to (Wiesenburg & Guinasso, 1979).

Text S5 Determination of stable carbon isotope values of CH₄ using GC-C-IRMS

Stable carbon isotope values of CH₄ in the headspace samples were analyzed by GC-C-IRMS. The GC-C-IRMS system consisted of a cryogenic preconcentration unit that was connected to a HP 6890N GC (Agilent Technologies, Santa Clara, USA) which is linked to the IRMS (Deltaplus XL, Thermo Finnigan, Bremen, Germany) by an oxidation reactor (ceramic tube, with oxygen activated Cu wire and /Ni/Pt wires serving as catalysts inside) and a GC Combustion III Interface (ThermoQuest Finnigan). For a detailed description of the δ¹³C-CH₄ measurements by GC-C-IRMS and technical details of the pre-concentration system, refer to previous studies by Althoff (2012), Comba et al. (2018) and Laukenmann et al. (2010). Ultra-pure carbon dioxide (carbon dioxide 4.5, Messer, Germany) was used as the monitoring gas. All δ¹³C-CH₄ values were normalized using two CH₄ standards (H-iso1 and B-iso1-standard, isometric instruments, Victoria, Canada) with values of -23.9 ± 0.2 ‰ and -54.5 ± 0.2 ‰ by two-scale anchor calibration according to Paul et al. (2007). The average standard deviation of the analytical measurements was in the range of 0.1 ‰ to 0.3 ‰ (based on three repeated measurements of CH₄ working standards). All δ¹³C-CH₄ values are expressed in the conventional δ notation, in permille (‰) vs. Vienna Pee Dee Belemnite (VPDB), using equation:

$$\delta^{13}C = \frac{\left(\frac{^{13}C}{^{12}C}\right)_{sample}}{\left(\frac{^{13}C}{^{12}C}\right)_{standard}} - 1 \quad \text{Eq. S3}$$

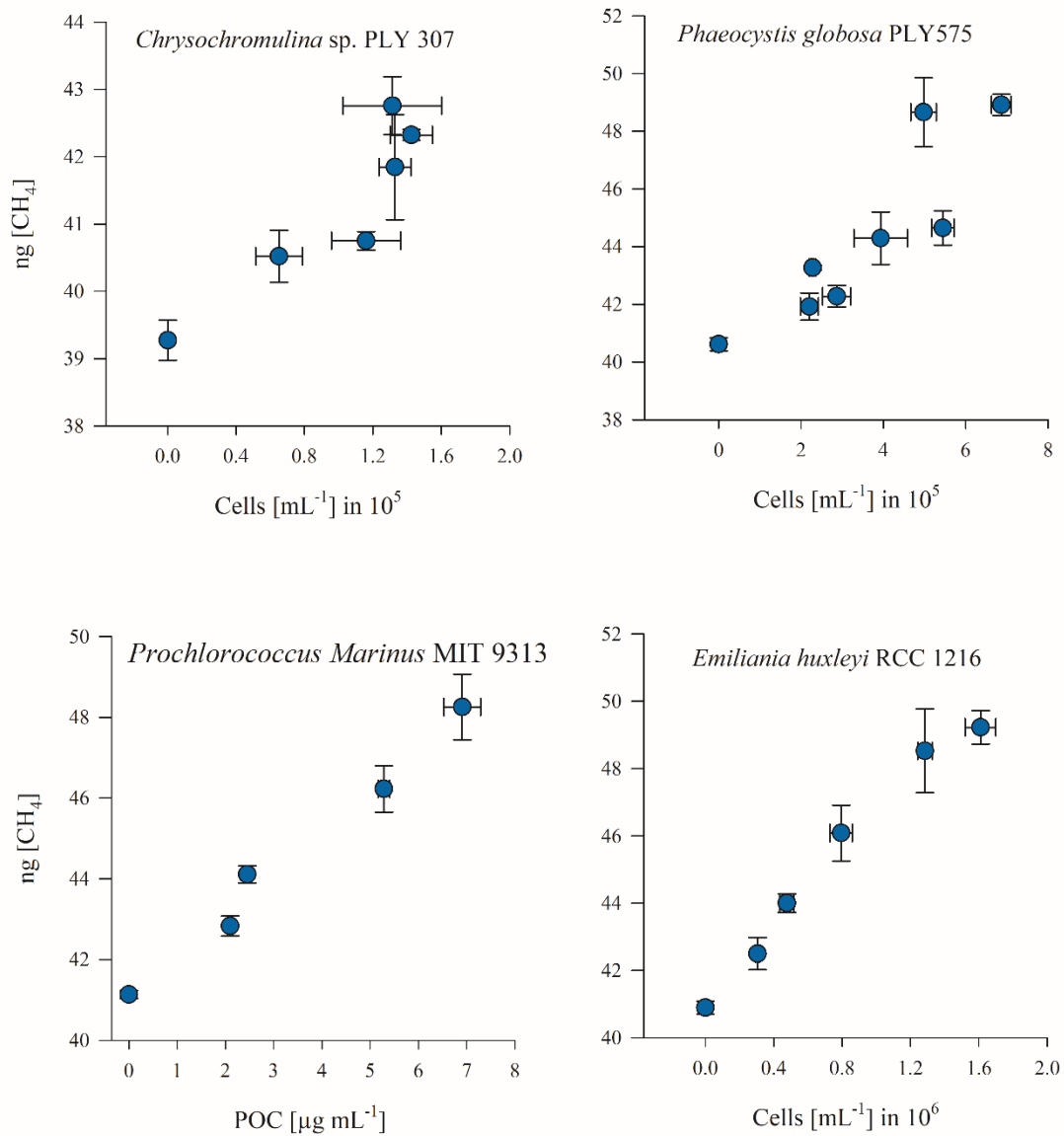


Figure S2. Correlation between CH_4 production and phytoplankton biomass. Please note that data for *Synechococcus* sp. are not shown. For these cultures, it was not possible to detach the biomass from the vessel wall without leaving any biomass residue.

Species	$\delta^{13}\text{C-POC}$ [‰]	n
<i>Chrysochromulina</i> sp.	-24.8 ± 1.5	9
<i>E. huxleyi</i>	-21.6 ± 0.6	9
<i>P. globosa</i>	-23.5 ± 0.4	11
<i>Prochlorococcus marinus</i> MIT 9313	-26.3 ± 0.3	10
<i>Synechococcus</i> WH 8102	-19.8 ± 0.4	10
<i>Synechococcus</i> WH 7803	-24.2 ± 0.7	10

Table S1. $\delta^{13}\text{C-POC}$ [‰] values of phytoplankton species.

Text S6 Determination of stable carbon isotope source values of CH_4 from previously published cyanobacterial incubation experiments.

We provide an additional dataset of calculated stable carbon isotope values of CH_4 emitted by cyanobacterial cultures. The experiments were performed in our laboratory and the $\delta^{13}\text{C-CH}_4$ values were previously published in Figure 1 in Bižić et al. (2020), while the corresponding CH_4 mass values were not included in the mentioned publication and are presented here for the first time as reciprocal values. A detailed methodological description can be found in Bižić et al. (2020). In short, the authors incubated cyanobacteria in flasks containing medium and headspace with ambient background CH_4 . The $\delta^{13}\text{C-CH}_4$ values and CH_4 mass within the headspace were determined at the end of incubation. In the present study, we generated Keeling plots using $\delta^{13}\text{C-CH}_4$ and CH_4 mass values of the treatments in which Bižić et al. (2020) cultured cyanobacteria with DIC corresponding to the natural abundance of ^{13}C ($\delta^{13}\text{C-DIC} = -4$ ‰, see text below for methodical description of DIC determination). This corresponds to treatments "M": non-inoculated growth medium and "C": Growth medium with cyanobacteria culture, in Figure 1 in Bižić et al., 2020. The Keeling plots and the resulting $\delta^{13}\text{C-CH}_{4,\text{source}}$ values are shown in Figure S3.

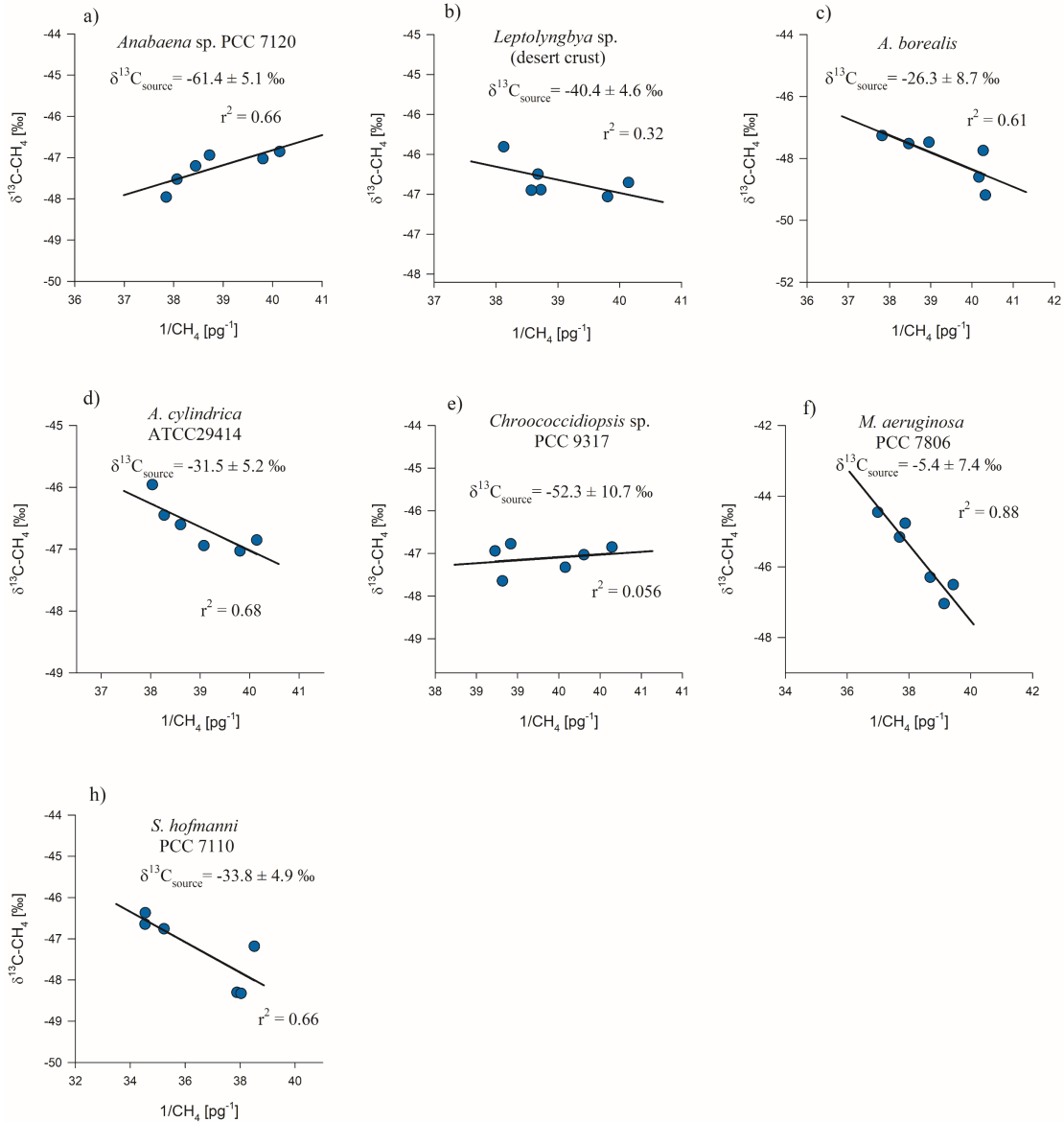


Figure S3. Keeling plots of five limnic cyanobacteria (a, c, d, f, g) and two terrestrial cyanobacterial species (b, e). $\delta^{13}C-CH_{4_source}$ values used to generate the Keeling plots were obtained from Bižić et al. (2020). The calculated $\delta^{13}C-CH_{4_source}$ values of each species are given by the extrapolated intercept with the y-axis CH_4 ($1/[CH_4] = 0$). The correlation between CH_4 mass (given as reciprocal) and the $\delta^{13}C-CH_4$ values of all incubations is shown in detail for each plot. The six data points are collected of each species are from independent incubation experiments.

Text S7 Determination of $\delta^{13}\text{C}$ -DIC values

We determined the $\delta^{13}\text{C}$ -DIC values of the culture medium (data were previously not shown in Bižić et al., 2020). To determine the isotopic composition of DIC, an aliquot of the medium (BG11 medium, Rippka et al. 1979, DIC = 0.4 mM, enriched by added NaHCO_3 ; pH 7.0) was transferred bubble-free into a 12 mL vial and sealed with a septum. The vial was inverted and a headspace of 8 mL N_2 was established using two syringe needles: N_2 gas flowed through one needle to introduce the headspace of the inverted vial, while displaced water exited the vial through the second needle. Afterwards, the entire DIC was converted into CO_2 by adding an excess of hydrochloric acid through the septum. To determinate $\delta^{13}\text{C}$ -DIC values, the $\delta^{13}\text{C}$ values of generated CO_2 were analyzed by transferring 2 mL headspace gas to the IRMS described above (Text S5). Deviating from this instrumental description, the sample was directly injected into the GC using an autosampler and was transferred to the IRMS under bypassing the oxidation reactor.

References:

- Bižić, M., Klintzsch, T., Ionescu, D., Hindiyeh, M. Y., Günthel, M., Muro-Pastor, A. M., et al. (2020). Aquatic and terrestrial cyanobacteria produce methane. *Science Advances*, 6(3), eaax5343.
<https://advances.sciencemag.org/content/advances/6/3/eaax5343.full.pdf>
- Craig, H. (1957). Isotopic standards for carbon and oxygen and correction factors for mass-spectrometric analysis of carbon dioxide. *Geochimica et Cosmochimica Acta*, 12(1), 133-149.
<https://www.sciencedirect.com/science/article/pii/0016703757900248>
- Keeling, C. D. (1958). The concentration and isotopic abundances of atmospheric carbon dioxide in rural areas. *Geochimica et Cosmochimica Acta*, 13(4), 322-334.
<http://www.sciencedirect.com/science/article/pii/0016703758900334>
- Kepler, F., Schiller, A., Ehehalt, R., Greule, M., Hartmann, J., & Polag, D. (2016). Stable isotope and high precision concentration measurements confirm that all humans produce and exhale methane. *Journal of Breath Research*, 10(1), 016003.
<http://stacks.iop.org/1752-7163/10/i=1/a=016003>
- Pataki, D. E., Ehleringer, J. R., Flanagan, L. B., Yakir, D., Bowling, D. R., Still, C. J., et al. (2003). The application and interpretation of Keeling plots in terrestrial carbon cycle research. *Global Biogeochemical Cycles*, 17(1), n/a-n/a.
<http://dx.doi.org/10.1029/2001GB001850>
- Paul, D., Skrzypek, G., & Fórizs, I. (2007). Normalization of measured stable isotopic compositions to isotope reference scales – a review. *Rapid Communications in Mass Spectrometry*, 21(18), 3006-3014. <http://dx.doi.org/10.1002/rem.3185>
- Rippka, R., Deruelles, J., Waterbury, J. B., Herdman, M., & Stanier, R. Y. (1979). Generic Assignments, Strain Histories and Properties of Pure Cultures of Cyanobacteria. *Microbiology*, 111(1), 1-61.
<https://www.microbiologyresearch.org/content/journal/micro/10.1099/00221287-111-1-1>
- Wiesenburg, D. A., & Guinasso, N. L. (1979). Equilibrium solubilities of methane, carbon monoxide, and hydrogen in water and sea water. *Journal of Chemical & Engineering Data*, 24(4), 356-360. <https://doi.org/10.1021/je60083a006>